Mem. S.A.It. Suppl. Vol. 5, 313

Memorie della
Supplementi

Simulating the cosmic web

L. Moscardini[1], M. Roncarelli[1], S. Borgani[2], A. Diaferio[3], K. Dolag[4], G. Murante[5], V. Springel[6], G. Tormen[4], L. Tornatore[2] and P. Tozzi[7]

[1] Dipartimento di Astronomia, Università di Bologna, via Ranzani 1, I-40127 Bologna, Italy e-mail: lauro.moscardini@unibo.it
[2] Dipartimento di Astronomia dell'Università di Trieste, via Tiepolo 11, I-34131 Trieste, Italy
[3] Dipartimento di Fisica Generale "Amedeo Avogadro", Università degli Studi di Torino, Torino, Italy
[4] Dipartimento di Astronomia, Università di Padova, vicolo dell'Osservatorio 2, I-35122 Padova, Italy
[5] INAF, Osservatorio Astronomico di Torino, Strada Osservatorio 20, I-10025 Pino Torinese, Italy
[6] Max-Planck-Institut für Astrophysik, Karl-Schwarzschild Strasse 1, Garching bei München, Germany
[7] INAF, Osservatorio Astronomico di Trieste, via Tiepolo 11, I-34131 Trieste, Italy

Abstract. We present results on the X–ray properties of clusters and groups of galaxies, extracted from a large cosmological hydrodynamical simulation assuming the concordance ΛCDM cosmological model. The simulation includes radiative cooling assuming zero metallicity, star formation and supernova feedback. We compute X–ray observables of the intra–cluster medium (ICM) for simulated groups and clusters and analyze their statistical properties. Finally we discuss the contribution of the warm/hot gas located in the cosmic web to the total backgrounds, considering both the (soft and hard) X-ray and millimetric (Sunyaev-Zel'dovich) band.

Key words. Cosmology: numerical simulations – galaxies: clusters – hydrodynamics – *X*–ray: galaxies

1. Introduction

To study the X-ray properties of galaxy clusters and the X-ray and millimetric emissions from the so-called cosmic web, we use the results obtained by analyzing a large-scale cosmological hydrodynamical simulation of a standard flat ΛCDM model, with matter density $\Omega_m = 0.3$, Hubble constant $H_0 = 70$ km s^{-1}Mpc^{-1}, baryon density $\Omega_{\rm bar} = 0.04$ and normalization of the power spectrum $\sigma_8 = 0.8$ [see Borgani et al. (2004) for more details]. The run was carried out with the TreeSPH code GADGET (Springel et al. 2001), by using 480^3 dark matter (DM) particles and as many gas particles. The box size was fixed to $192\,h^{-1}$Mpc; the corresponding mass resolu-

Send offprint requests to: L. Moscardini
Correspondence to: Dipartimento di Astronomia, via Ranzani 1, I-40127 Bologna, Italy

tion is $m_{DM} = 4.62 \times 10^9 h^{-1} M_\odot$ and $m_{\rm gas} = 6.93 \times 10^8 h^{-1} M_\odot$; the Plummer-equivalent softening length was $7.5 h^{-1}$ comoving kpc. The simulation includes, besides gravity and hydrodynamics, an accurate treatment of different physical processes acting on the intracluster medium, like star formation processes (by adopting a sub-resolution multiphase model for the interstellar medium), feedback from supernovae with the effect of weak galactic outflows, radiative gas cooling and, finally, heating by a uniform, time-dependent, photoionizing UV background. In total the simulation required about 40,000 CPU hours on 64 processors of the IBM-SP4 computer located at CINECA. We produced 100 snapshots (corresponding to 1.2 Tb of data) logarithmically equispaced between $z = 9$ and the present time.

2. The X-ray properties of galaxy clusters and groups

Clusters and groups of galaxies have been identified by using a standard friends-of-friends algorithm, adopting a linking length of 0.15 times the mean DM interparticle separation. At $z = 0$ we identified 117 cluster with mass larger than $10^{14} h^{-1} M_\odot$. The largest structure we found has an emission-weighted temperature of $T \approx 7$ keV. The simulation contains 72 objects with $T > 2$ keV, out of which 23 have $T > 3$ keV. This very large sample of simulated clusters and groups that are represented with good enough numerical resolution allows us to obtain reliable estimates of the X-ray observable quantities, such as luminosity, temperature and entropy. An extended analysis of the X-ray properties of our clusters at $z = 0$ and at $z \geq 0.5$ can be found in Borgani et al. (2004) and in Ettori et al. (2004), respectively. Here we summarize only the most interesting results and refer the reader to the quoted papers for a more complete discussion.

In the left panel of Fig. 1, we compare the observed and the simulated M–T relation, computed at $\bar{\rho}/\rho_c = 500$. The cluster masses are estimated by reproducing the procedure followed by Finoguenov et al. (2001). In particular the equation of hydrostatic equilibrium is applied after fitting the gas density profile to a β–model and assuming a polytropic equation of state. The simulation results show a good agreement with the observed relation. Notice that if we compute the mass directly from the simulation without following the observational procedure we find a normalisation which is about 20 per cent higher. This result indicates that possible biases in the observational mass estimates, related to the assumptions of β–model profile and hydrostatic equilibrium [see also the discussion by Rasia et al. (2004)], may originate differences between simulated and observed M–T relations.

In the right panel of Fig. 1, we compare the observed and simulated relations between bolometric luminosity, L_X, and emission–weighted temperature, $T_{\rm ew}$. The latter has been computed weighting the contribution from each gas particle according to its emissivity in the [0.5-10] keV energy band. We found that the simulated L_X–T relation provides a good fit to data at $T \gtrsim 2$ keV, while it does not produce any steepening at the scale of groups (Lloyd-Davies et al. 2000). Notice that a recent analysis by Osmond & Ponman (2004) actually demonstrates that the present quality of data is not good enough to allow a precise determination of the L_X–T scaling for galaxy groups.

Not all the results from the simulation are in good agreement with the corresponding observational data. For example, the temperature profiles are discrepant: while their shape in the outer regions, at $R \gtrsim 0.3 R_{180}$, is similar to the observed one, simulation profiles are steadily increasing towards the centers, with no evidence for an isothermal regime followed by a smooth decline at $R \lesssim 0.3\, R_{2500}$. The entropy properties of simulated clusters are also quite different from observational results. In the outer regions, the entropy profiles from the simulation are remarkably self–similar, while observations show evidence for excess entropy at the scale of groups (Ponman et al. 2003). In the inner regions, we detect a significant excess entropy whose amount is almost independent of the cluster temperature. Although the resulting S–T relation therefore deviates from the self–similar expectation, it is anyway steeper than observed. Finally the fraction of baryons which cool and turn into stars within the virial

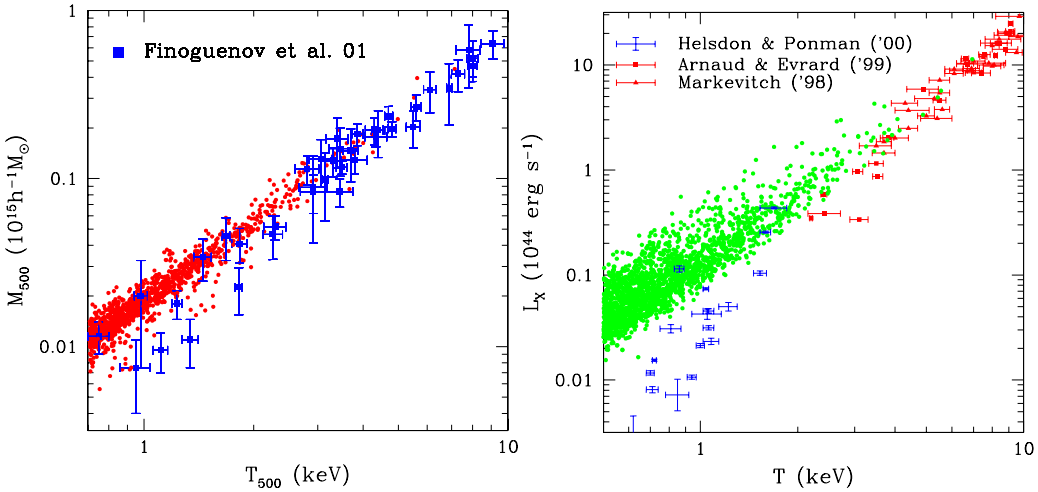

Fig. 1. Left panel: Comparison between the observed (blue filled squares) and the simulated (red dots) M–T relation, computed at $\bar{\rho}/\rho_c = 500$. Right panel: Comparison between the observed (red and blue dots) and the simulated (green dots) $L_X - T$.

regions of clusters is $f_* \simeq 20$ per cent, with a slight tendency to be higher for colder systems. This value is substantially smaller than the one found in simulations that do not include efficient feedback mechanisms, but it is still higher than observed by about a factor of two (Lin et al. 2003).

In general, these results show that the physical processes included in our simulation are able to account for the basic global properties of clusters, such as the scaling relations between mass, temperature and luminosity. At the same time, we find indications suggesting that a more efficient way of providing non–gravitational heating from feedback energy compared to what is implemented in the simulation is required: this 'extra heating' should not only reduce the amount of gas that cools, but also needs to 'soften' the gas density profiles of poor clusters and groups by increasing the entropy of the relevant gas.

3. The contributions to backgrounds from the cosmic web

In this Section we want to compare our numerical results to other datasets, particularly those involving the emission properties of the diffuse gas. Recent results from deep Chandra observations (Brandt et al. 2001; Rosati et al. 2002) have shown that the contribution to the X-ray background from diffuse baryons in the soft band [0.5-2 keV] cannot exceed $(2-4)\times10^{-13}$ erg s^{-1} cm^{-2} deg^{-2}. As discussed by Voit & Bryan (2001), this upper limit can be used to further constrain the models aimed at describing the physical processes in the gas component, like the one included in our simulation. Moreover, the intensity and the spatial distribution of the signal produced in the millimetric band by the SZ effect, i.e. the Compton scattering of the photons of the cosmic microwave background with the electrons associated with the gas in the warm/hot phase (the so-called WHIM), strongly depend on the thermal history of baryons. Therefore our simulation can be used to estimate the expected background from diffuse, ionized baryons. Unfortunately the best observation to date only allow to set an upper limit to the mean comptonisation parameter [$y < 1.5 \times 10^{-5}$, obtained by the COBE/FIRAS experiment; Fixen et al. (1996)].

Following the work of Croft et al. (2001), we developed and implemented a software aimed at extracting the past-light cone, from

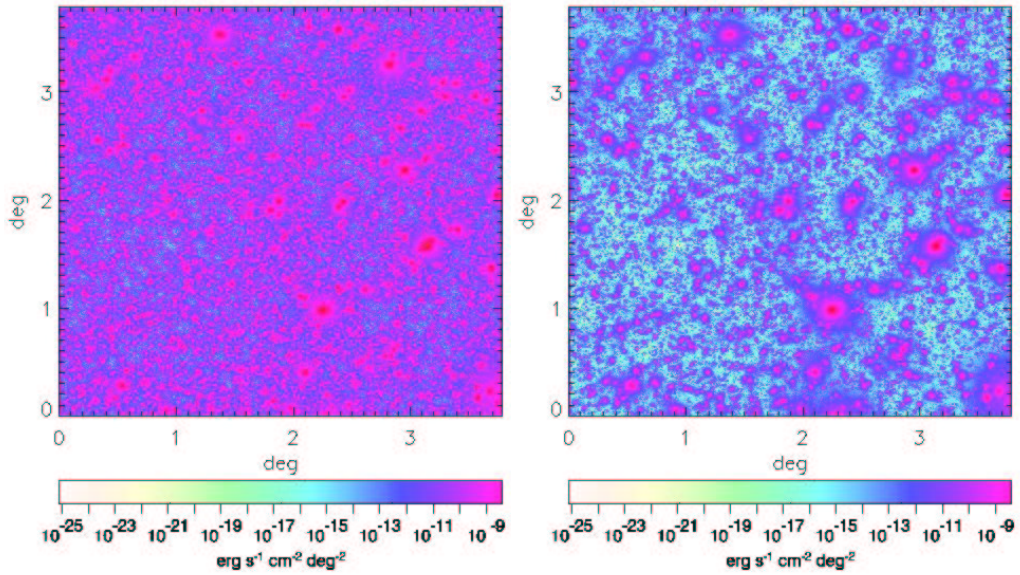

Fig. 2. Maps of the diffuse emission intensity in the soft band (left panel) and hard band (right panel).

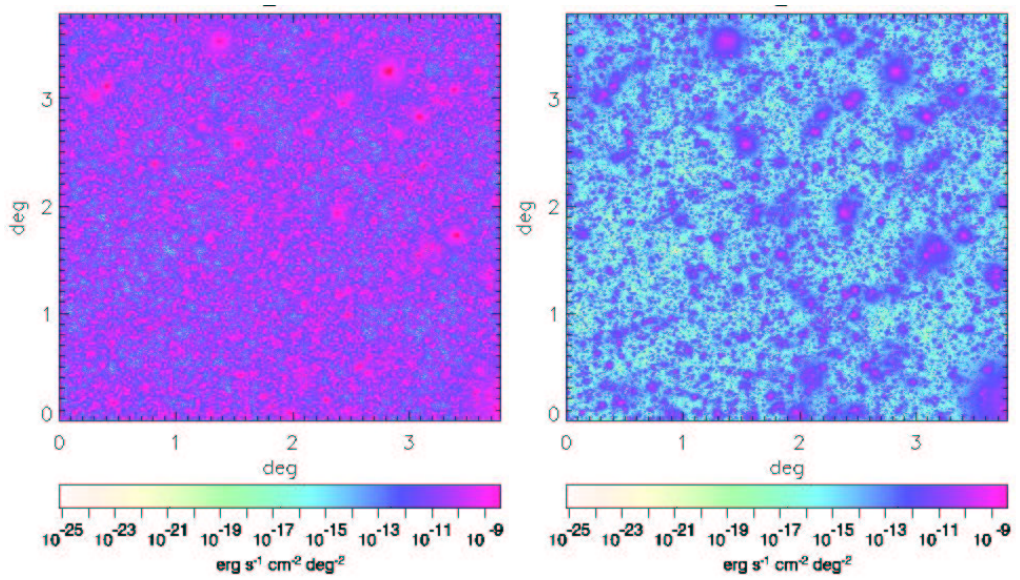

Fig. 3. As Fig. 2, but for the emission from the WHIM.

the numerical experiment by stacking the different outputs while avoiding spurious spatial alignments thanks to random recenterings and reflections of the particle coordinates. We started the production of an extended set of realistic X-ray maps, by considering the emission both in the soft [0.5-2 keV] and in the hard [2-10 keV] X-ray bands. Given the large box-

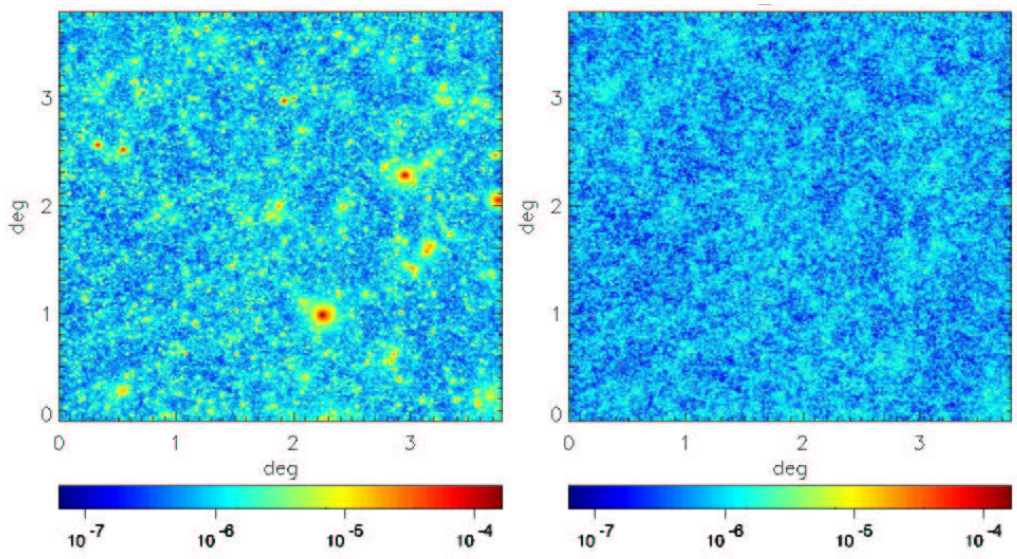

Fig. 4. Maps of the thermal SZ effect. The total signal and the signal coming from the WHIM only, are shown in the left and right panels, respectively.

size of the simulation, each map covers almost 15 square degrees, thanks to the duplication of the original boxes at large redshifts. An example of these maps is shown in Fig. 2, where left and right panels refer to the total emission in the soft and hard bands, respectively.

As said, one of our main goals is to estimate the contribution of the X-ray emission from the WHIM located in the filaments to the total background. For this purpose, we isolated the emission from gas particles having a temperature between 10^5 and 10^7 K. The resulting map, for the same realization shown in Fig. 2, is presented in Fig. 3. Again the results for the soft and hard bands are shown in the left and right panels, respectively. To characterize the X-ray background in Roncarelli et al. (2004) we are computing different statistics, like the mean X-ray background intensity contributed by both galaxy clusters and IGM, the redshift distribution of the signal and its hardness ratio, i.e. the ratio between the emission in the hard and soft bands. All the above quantities can be directly compared to the datasets obtained from deep surveys, thus providing constraints on the various processes affecting the gas component and their relative importance. In particular, for the realization shown in the previous figures, we found that the WHIM has a contribution of 1.2×10^{-12} (1.6×10^{-14}) erg s^{-1} cm^{-2} deg^{-2}, in the soft (hard) bands; the total X-ray emission (i.e. including the hot gas in galaxy clusters) is approximately 3 (50) times larger. These values, if confirmed by a more robust statistical analysis, could create a further problem to the model for the gas physics included in our simulation.

At the same time we are producing a set of maps showing the emission in the millimetric band produced by the thermal SZ effect. The linear relation between the SZ emissivity and gas density allows us to trace the thermal history of the hot gas in dark haloes and filaments, i.e. in a density environment that is complementary to that where the diffuse X-ray emission comes from. In this respect our hydrodynamical simulation, characterized by its large computational box and sophisticated treatment of the gas physics, constitutes a significant improvement with respect to previous similar analyses (White et al. 2002; da Silva et

al. 2004). The SZ map obtained from the same realization is shown in Fig. 4.

4. Conclusions

Our cosmological simulation shows an encouraging agreement with some of the most important observed X-ray cluster properties, like e.g. the mass-temperature and luminosity-temperature relations. However, there are also a number of discrepancies that remain unaccounted for (e.g. temperature and entropy profiles). This suggests the need for yet more efficient sources of energy feedback and/or the need to consider additional physical process which may be able to further suppress the gas density at the scale of poor clusters and groups, and, at the same time, to regulate the cooling of the ICM in central regions.

Acknowledgements. The simulation has been realized using the IBM-SP4 machine at the "Centro Interuniversitario del Nord-Est per il Calcolo Elettronico" (CINECA, Bologna), with CPU time assigned thanks to an INAF–CINECA grant.

References

Borgani S. et al., 2004, MNRAS, 348, 1078
Brandt P.C. et al., 2001, AJ, 122, 1
Croft R.A.C., Di Matteo T., Davè R., Hernquist L., Katz N., Fardal M.A., Weinberg D.H., 2001, ApJ, 557, 67
da Silva A.C., Kay S.T., Liddle A.R., Thomas P.A., 2004, MNRAS, 348, 1401
Ettori S. et al., 2004, MNRAS, in press
Finoguenov A., Arnaud M., David L.P., 2001, ApJ, 555, 191
Fixsen D.J. et al., 1996, ApJ, 473, 576
Lin Y.-T., Mohr, J.J., Stanford S.A., 2003, ApJ, 591, 749
Lloyd-Davies E.J., Ponman T.J., Cannon D.B., 2000, MNRAS, 315, 689
Osmond J.P.F., Ponman T.J., 2004, MNRAS, 350, 1511
Ponman T.J., Sanderson A.J.R., Finoguenov A., 2003, MNRAS, 343, 331
Rasia E., Tormen G., Moscardini L., 2004, MNRAS, 351, 237
Roncarelli M. et al., 2004, in preparation
Rosati P. et al. 2002, ApJ, 566, 667
Springel V., Yoshida N., White S.D.M., 2001, NewA, 6, 79
Voit G.M., Bryan G.L., 2001, ApJ, 551, L139
White M., Hernquist L., Springel V., 2002, ApJ, 579, 16